drugs and drug candidates

MDPI

Article

Synthesis, In Vitro Antitumor Activity, and In Silico ADMET Evaluation of β-Lapachone-Based Thiosemicarbazones

Elizabete Silva de Sousa [1], Edilane Almeida da Silva [1], Délis Galvão Guimarães [2], Ingrid Louise Santos de Souza [2], Arlan de Assis Gonsalves [3], Paulo Michel Pinheiro Ferreira [4], Rayran Walter Ramos de Sousa [4], Marcília Pinheiro da Costa [5] and Cleônia Roberta Melo Araújo [1,*]

1 Postgraduate in Health and Biological Sciences, Federal University of the São Francisco Valley, Petrolina 56304-917, Brazil; elizabete.sousa@discente.univasf.edu.br (E.S.d.S.); edilane.almeida@discente.univasf.edu.br (E.A.d.S.)
2 Pharmacy School, Federal University of the São Francisco Valley, Petrolina 56304-917, Brazil; delisgalvao@gmail.com (D.G.G.); ingrid.louise@discente.univasf.edu.br (I.L.S.d.S.)
3 Postgraduate in Materials Science, Federal University of the São Francisco Valley, Petrolina 56304-917, Brazil; arlan.gonsalves@univasf.edu.br
4 Laboratory of Experimental Cancerology (LabCancer), Department of Biophysics and Physiology, Federal University of Piauí, Teresina 64049-550, Brazil; pmpf@ufpi.edu.br (P.M.P.F.); rayran.ramos@hotmail.com (R.W.R.d.S.)
5 Postgraduate in Pharmaceutical Sciences, Federal University of Piauí, Teresina 64049-550, Brazil; marciliapc@ufpi.edu.br
* Correspondence: cleonia.araujo@univasf.edu.br

Abstract

Background/Objectives: β-Lapachone and triapine are compounds with recognized antitumor potential—the former is an *ortho*-naphthoquinone, and the latter a thiosemicarbazone inhibitor of ribonucleotide reductase. This study aimed to synthesize and evaluate new β-lapachone-based thiosemicarbazones (**TSC1**–**TSC6**) as potential antineoplastic agents. **Methods**: Lapachol was isolated from *Tabebuia* sp. and used to obtain *ortho*-naphthoquinones (**2**–**4**), which served as precursors for thiosemicarbazones (**TSC1**–**TSC6**). NMR and HRMS spectra were used to characterize the compounds. Their cytotoxic activity was evaluated in vitro against murine melanoma (B16–F10), colon carcinoma (CT26.WT), and breast cancer (4T1) cell lines, as well as normal fibroblasts (L929). Pharmacokinetic parameters were predicted in silico using ADMETLab 3.0. **Results**: β-Lapachone exhibited strong cytotoxicity toward tumor cells with moderate effects on normal cells, while thiosemicarbazones of β-lapachone, **TSC1**, and **TSC3** demonstrated lower potency but greater selectivity. The β-lapachone-3-sulfonic acid showed high activity against melanoma and breast cancer cells and low toxicity toward normal cells, indicating tumor selectivity. In contrast, their thiosemicarbazones, **TSC2**, **TSC4**, and **TSC6**, showed weak or no antiproliferative activity. The 3-iodo-β-lapachone was cytotoxic to both tumor and normal cells, whereas its derivative **TSC5** demonstrated moderate activity with reduced toxicity. β-Lapachone, β-lapachone-3-sulfonic acid, **TSC1**, and **TSC3** exhibited favorable ADME profiles (QED ≈ 0.61–0.66), suggesting good oral bioavailability. **Conclusions**: The β-lapachone-3-sulfonic acid and the β-lapachone-based thiosemicarbazones **TSC1** and **TSC3** emerged as promising lead candidates, combining tumor selectivity, favorable pharmacokinetic properties, and structural innovation for the development of safer and more effective antineoplastic agents.

Keywords: β-lapachone; β-lapachone-3-sulfonic acid; cytotoxicity; naphthoquinone; 3-iodo-β-lapachone

Check for updates

Academic Editor: Jean Jacques Vanden Eynde

Received: 17 November 2025
Revised: 10 December 2025
Accepted: 18 December 2025
Published: 21 December 2025

Copyright: © 2025 by the authors. Licensee MDPI, Basel, Switzerland. This article is an open access article distributed under the terms and conditions of the Creative Commons Attribution (CC BY) license.

1. Introduction

The search for more effective and safer anticancer drugs remains one of the greatest challenges in pharmaceutical R&D. In 2024, the U.S. Food and Drug Administration (FDA) approved 50 novel drug therapies, approximately 30% of which were indicated for the treatment of neoplastic diseases [1]. However, the development of new drugs continues to face significant challenges, with a high rate of failure in phase I and II clinical trials. Between 2013 and 2015, anticancer agents exhibited an estimated failure rate of 32%, making oncology the therapeutic area with the highest attrition during these stages [2]. Introducing pharmacokinetic studies in the early phases of drug development has been proposed as an effective strategy to reduce late-stage failures, as these studies provide critical insights into drug absorption, distribution, metabolism, and excretion (ADME), allowing early identification of candidates with unfavorable pharmacological profiles [3].

β-Lapachone is a naphthoquinone with well-recognized antitumor potential that can be readily obtained through the acid-catalyzed cyclization of lapachol [4], Figure 1. However, it was originally isolated from the heartwood of *Handroanthus impetiginosus* [5]. The antitumor mechanism of β-lapachone has been extensively investigated. Studies by Li et al. (2003) and Seville et al. (2005) demonstrated that β-lapachone rapidly increases the levels of the transcription factor E2F-1, thereby triggering checkpoint-mediated selective apoptosis in tumor cells without affecting normal cells [6,7]. The biotechnology company ArQule evaluated β-lapachone (ArQ-501) as an anticancer agent in phase I and II clinical trials, where the compound was well tolerated [8–10]. Subsequently, in 2007, Khong et al. reported pancreatic adenocarcinoma regression when β-lapachone was administered in combination with gentamicin in adult patients with previously untreated non-resectable pancreatic adenocarcinoma [11].

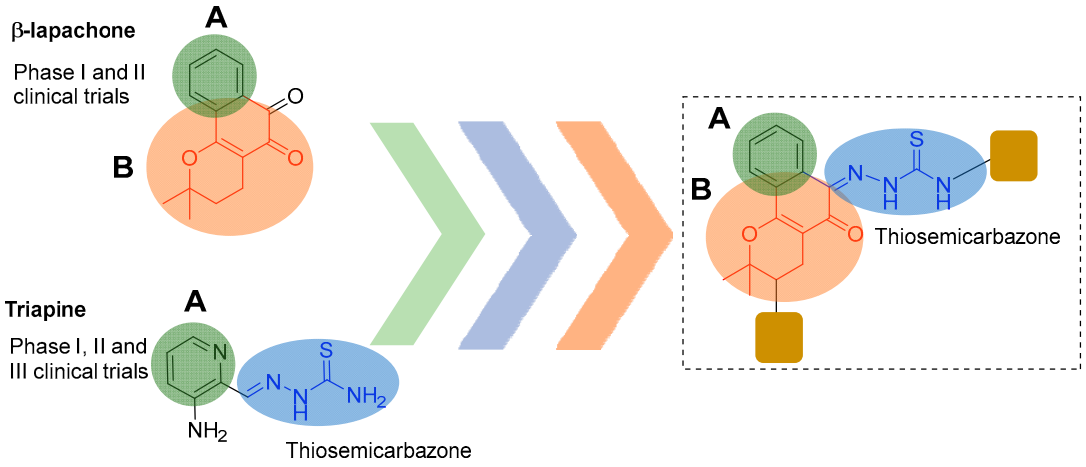


Figure 1. Schematic representation of the structural design of β-lapachone-based thiosemicarbazones (**TSC1**–**TSC6**). **A**-The aromatic ring present in both β-lapachone and triapine and **B**-The ring system present in β-lapachone.

Triapine is a thiosemicarbazone that has been evaluated in phase I [12], II [13], and III [14] clinical trials for cancer treatment, Figure 1. Its mechanism of action is associated with the inhibition of the enzyme ribonucleotide reductase, and it has been suggested that its metal-chelating ability—a characteristic feature of the thiosemicarbazone group—plays a key role in its bioactivity. In phase I clinical trials, Kunos et al. (2017) reported that the combination of triapine with radiotherapy and cisplatin resulted in high clinical response rates in women with cervical and vaginal cancers [12]. In phase II studies, Zeidner et al. (2014) investigated the activity of triapine combined with fludarabine in patients with

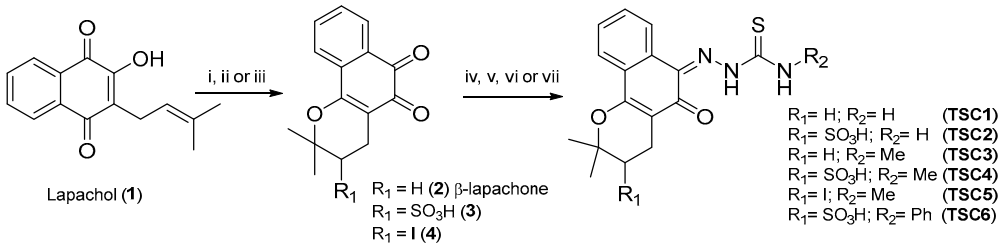
myeloproliferative neoplasms, reporting a 29% increase in complete or partial response rates [15].

Considering the antitumor potential of β-lapachone and triapine, a series of novel β-lapachone-based thiosemicarbazones was rationally designed, preserving the aromatic ring A present in both compounds, the B region of the *ortho*-naphthoquinone, and the thiosemicarbazone moiety from triapine. The thiosemicarbazones were synthesized, their antitumor activities were evaluated in vitro, and their ADME properties were investigated in silico, Figure 1.

2. Results and Discussion

2.1. Synthesis

The proposed synthetic route employs lapachol (**1**) as the starting material. Initially, the natural naphthoquinone was extracted from the heartwood shavings of yellow ipe (*Tabebuia* sp.) through an acid–base extraction method, affording a 1.5% (*w*/*w*) yield [16]. β-lapachone (**2**) and β-lapachone-3-sulfonic acid (**3**) were synthesized via acid-catalyzed cyclization of naphthoquinone **1**, with yields of 95% and 80% using concentrated H_2SO_4 and Ac_2O/H_2SO_4, respectively [17]. For the synthesis of 3-iodo-β-lapachone (**4**), obtained in 20% yield, lapachol (**1**) was subjected to an iodo-cyclization reaction employing iodo and pyridine as catalyst [17] (Scheme 1).



Scheme 1. Synthetic route to obtain the *ortho*-naphthoquinones (**2**–**4**) and thiosemicarbazones (**TSC1**–**TSC6**) employed the lapachol (**1**). The numbers (i–vii) above the arrows indicate the reactants and solvents used in each chemical reaction, as shown in the scheme.

The thiosemicarbazones were obtained in yields ranging from 13 to 87%, and their structures were confirmed through the analysis of one- and two-dimensional Nuclear Magnetic Resonance (NMR) spectra, as well as by mass spectrometry data (Figures S1–S9). The spectra of all thiosemicarbazones showed signal integration and multiplicity patterns (spin–spin splitting) consistent with their molecular structures. In addition, the ^{1}H NMR spectra (400 MHz, DMSO-d_6 or $CDCl_3$) of all compounds (**TSC1**–**TSC6**) displayed a singlet integrating for one hydrogen atom in the δH 14.9–15.3 region (C=N–NH). This signal, with a high chemical shift value, is characteristic of the formation of an intramolecular hydrogen bond between the hydrogen atom of the hydrazone functional group and the oxygen atom of the ketonic carbonyl group. The presence of this intramolecular hydrogen bond suggests that the thiosemicarbazones (**TSC1**–**TSC6**) were obtained with the C=N double bond of the hydrazone moiety in the Z configuration [18]. Furthermore, the ^{13}C NMR spectra (100 MHz, DMSO-d_6 or $CDCl_3$) of all thiosemicarbazones exhibited a single signal for the ketonic carbonyl carbon in the δC 179.6–181.2 range, suggesting nucleophilic addition to one of the carbonyl groups of the *ortho*-naphthoquinones. Signals corresponding to carbons C6 (C=N–NH) and C13 (C=S) were also observed in the δC 126.4–130.2 and δC 177.8–180.9 regions, respectively [18].

2.2. Antitumor Activity

To investigate the bioactive potential of the synthesized compounds, cytotoxicity assays were performed against three tumor cell lines: murine melanoma (B16–F10), murine colon carcinoma (CT26.WT), and murine breast cancer (4T1). In addition, the cytotoxic activity of the compounds was also evaluated against a normal cell line, mouse fibroblasts (L929).

In this assay, the cytotoxic potential was assessed through the antiproliferative activity of the *ortho*-naphthoquinones (**2**–**4**) and thiosemicarbazones (**TSC1**–**TSC6**) at a concentration of 25 μg/mL (Table S1). Doxorubicin was used as a positive control at 0.5 μg/mL, and exhibited inhibition ranging from 46.41% to 60.18% against the evaluated tumor cell lines. β-Lapachone (**2**) is a well-known antitumor compound that has been evaluated in phase I and II clinical trials, either alone or in combination with other antineoplastic agents, showing antitumor activity, toxicological safety, and pharmacokinetic efficacy [8–11,19]. In this study, the activity of naphthoquinone **2** was assessed for comparison with its synthetic derivatives. Compound **2** inhibited cell proliferation by more than 90% in the B16–F10 and CT26.WT tumor cell lines, as well as 82.25% in 4T1, while displaying moderate cytotoxicity toward normal L929 cells (67.75%), Table 1.

Table 1. Inhibition of cellular proliferation by naphthoquinones (**2**–**4**) and thiosemicarbazones (**TSC1**–**TSC6**) against tumor and normal cell lines.

Compound	Cell Proliferation Inhibition (%)			
	B16–F10	**4T1**	**CT26.WT**	**L929**
2	94.68 ± 0.40 *	82.25 ± 2.39 *	91.27 ± 0.86 *	67.75 ± 6.65 *
3	84.41 ± 0.23 *	68.36 ± 3.29 *	7.69 ± 1.61	28.84 ± 8.10
4	93.19 ± 0.53 *	78.18 ± 4.31 *	86.88 ± 7.23 *	78.46 ± 6.58 *
TSC1	53.90 ± 1.48	38.38 ± 5.09	0.00 ± 9.62	4.67 ± 10.35
TSC2	37.60 ± 3.85 *	0.00 ± 8.16	13.15 ± 5.88 *	0.00 ± 3.60
TSC3	75.27 ± 1.59 *	66.42 ± 4.18 *	0.00 ± 2.41	37.95 ± 4.85 *
TSC4	29.29 ± 2.53 *	0.00 ± 5.68	6.05 ± 10.39	12.97 ± 4.33
TSC5	57.85 ± 4.44 *	22.94 ± 4.94 *	0.36 ± 7.68	12.17 ± 2.33
TSC6	31.21 ± 1.39 *	00.00 ± 4.31	24.82 ± 1.20 *	0.00 ± 18.59
Doxorubicin	58.90 ± 3.40 *	46.41 ± 0.68 *	60.18 ± 4.84 *	18.40 ± 4.27 *

Values are expressed as mean ± standard deviation (SD) of three independent experiments. The positive control was doxorubicin (0.5 μg/mL). * $p < 0.05$ compared to control by one-way ANOVA followed by Dunnett's post hoc test.

TSC1 and **TSC3** are thiosemicarbazone derivatives of naphthoquinone **2**. Both compounds inhibited the proliferation of tumor cell lines less potently than compound **2**. **TSC1** exhibited moderate activity against B16–F10 (53.9%) cell line, with low cytotoxicity toward the normal fibroblast line (4.67%), indicating a profile of low toxicity and high safety, in contrast to the moderate cytotoxicity of compound **2** against L929 cells. **TSC3** also showed higher activity against melanoma and breast cancer cell lines, inhibiting cell proliferation by 75.27% and 66.42%, respectively (Table 1).

β-Lapachone-3-sulfonic acid (**3**) inhibited the proliferation of melanoma and breast cancer cells by 84.41% and 68.36%, respectively, while exhibiting minimal activity against CT26.WT (7.69%) and low toxicity toward normal cells (28.84%). This behavior suggests tumor selectivity, possibly associated with differences in mechanisms of action or cellular permeability among cell lines of distinct origins.

Thiosemicarbazones **TSC2**, **TSC4**, and **TSC6**, which are derivatives of naphthoquinone **3**, showed reduced or no antiproliferative activity against all tested cell lines, with inhibition below 40% and no significant effect on normal cells, classifying them as compounds with low cytotoxic potency. Therefore, β-lapachone-3-sulfonic acid (**3**) can be considered a

promising candidate, as it combines significant activity against specific malignant cell lines with low toxicity toward non-tumor cells.

3-Iodo-β-lapachone (**4**) exhibited a behavior similar to that of naphthoquinone **2**, showing inhibition rates of 93.19%, 78.18%, and 86.88% against melanoma, breast cancer, and colon cancer cell lines, respectively. This effect is comparable to that of doxorubicin (58.9–60.2%) in the tested cell lines. However, a high level of cytotoxicity toward normal cells (78.46%) was also observed, suggesting low selectivity.

TSC5, the thiosemicarbazone derivative of naphthoquinone **4**, displayed moderate antiproliferative activity against melanoma cells (57.85%), with low cytotoxicity toward the normal fibroblast line (12.97%), indicating a profile of low toxicity and greater safety. The introduction of the methylthiosemicarbazone moiety appears to have conferred selectivity, Table 1.

The results indicated that, except for **TSC6**, all synthesized compounds displayed cytotoxic activity against at least one of the evaluated cancer cell lines, supporting their potential as promising scaffolds for the development of new antineoplastic agents.

2.3. In Silico ADMET Prediction

In silico evaluation of ADMET properties represents an important step in the screening of drug candidate compounds, allowing the prediction of parameters related to absorption, distribution, metabolism, excretion, and toxicity [20,21]. The results obtained using ADMETLab 3.0 for the *ortho*-naphthoquinones (**2**–**4**) and thiosemicarbazones (**TSC1**–**TSC6**) (Table 2) revealed differences in solubility, lipophilicity, permeability, and drug-likeness, reflecting distinct pharmacokinetic potentials.

Table 2. Predicted physicochemical and pharmacokinetic properties of naphthoquinones (**2**–**4**) and thiosemicarbazones (**TSC1**–**TSC6**).

Compound	MW	logS	logP	TPSA	QED	Caco-2	HIA	PPB	CL_{plasma}	MEC-18
2	242.09	−4.164	2.472	43.370	0.657	−4.572	0.787	98.442	6.353	41.400
3	322.05	−2.430	1.285	97.740	0.623	−4.832	0.964	98.463	1.559	72.600
4	367.99	−4.595	2.963	43.370	0.402	−4.506	0.937	98.185	5.937	62.700
TSC1	315.10	−4.177	2.659	76.710	0.613	−5.297	0.000	98.629	2.072	43.429
TSC2	395.06	−3.689	1.427	131.08	0.384	−5.780	0.001	98.476	0.886	75.571
TSC3	329.12	−4.263	2.933	62.720	0.612	−5.110	0.005	98.639	4.150	42.957
TSC4	409.08	−3.387	0.945	117.09	0.379	−5.694	0.068	98.626	1.336	75.000
TSC5	455.02	−4.592	3.173	62.720	0.295	−5.118	0.017	98.553	4.291	65.217
TSC6	471.09	−5.389	2.993	117.09	0.355	−5.544	0.008	98.523	0.608	87.000

Molecular weight (MW), solubility (logS), lipophilicity (logP), topological polar surface area (TPSA), and quantitative estimate of drug-likeness (QED), minimum energy conformation at 18 descriptors (MEC-18), Caco-2 permeability, human intestinal absorption (HIA), plasma protein binding (PPB, %), and plasma clearance (CL_{plasma}) were calculated using predictive computational tools.

The quantitative estimate of drug-likeness (QED), developed by Bickerton et al., 2012, is an index designed to quantitatively assess the degree to which a molecule resembles approved drugs in terms of its physicochemical properties [22]. The QED expresses an optimal balance of molecular features associated with favorable oral bioavailability.

Compounds **2**, **3**, **TSC1**, and **TSC3** exhibited the highest QED values (0.612–0.657), indicating a favorable combination of molecular weight (MW < 330 Da), topological polar surface area (TPSA < 100 $Å^2$), and moderate lipophilicity (logP ≈ 2–3), Table 2. These characteristics suggest good oral bioavailability, consistent with Lipinski's Rule of Five [23].

Compounds **2** and **TSC3** showed favorable logP values (2.47–2.93) and adequate solubility (logS ≈ −4), which support good oral absorption and passive diffusion across biological membranes. The thiosemicarbazone **TSC1** did not exhibit suitable HIA and

Caco-2 values, indicating poor absorption; however, it presented favorable logS (−4.177) and logP (2.659) values (Table 2).

Naphthoquinone **3** stood out for its high human intestinal absorption (HIA = 0.964) and Caco-2 permeability consistent with absorbable compounds (−4.83). Despite its relatively low solubility (logS = −2.43) and greater polarity (TPSA = 97.7 Å^2) (Table 2), its overall profile suggests a good balance between solubility and permeability, making β-lapachone-3-sulfonic acid (**3**) a promising candidate.

Compounds **4**, **TSC2**, **TSC4**, **TSC5**, and **TSC6** exhibited low QED values (0.29–0.40). **TSC2**, **TSC4**, and **TSC6** showed TPSA values above 110 Å^2, which tends to limit intestinal permeability and cellular uptake [24]. In addition, the low intestinal absorption (HIA < 0.1) observed for **TSC2**, **TSC4**, **TSC5**, and **TSC6** indicates a less favorable pharmacokinetic profile, possibly resulting from their high polarity and molecular weight (>400 Da). Regarding 3-iodo-β-lapachone (**4**), despite its borderline QED value, it presented acceptable logS, logP, TPSA, and HIA parameters for oral administration (Table 2).

In terms of plasma clearance (CL_{plasma}), compounds with higher lipophilicity and lower TPSA (such as **2**, **4**, and **TSC5**) exhibited higher clearance values (5–6 mL/min/kg), suggesting faster elimination. In contrast, more polar and higher-molecular-weight molecules (**TSC2**, **TSC4**, and **TSC6**) showed reduced CL_{plasma} (<1.5 mL/min/kg), which may favor a prolonged half-life.

In addition to the classical ADME parameters, the medicinal chemistry evolution 2018 (MEC-18) descriptor was incorporated as a criterion for structural lead-likeness. MEC-18 quantifies the three-dimensional complexity and the 'novelty' of the molecular scaffold, with values ≥45 indicating high complexity and compatibility with modern medicinal chemistry principles [25].

TSC2, **TSC4**, **TSC5**, and **TSC6** displayed high MEC-18 values but unfavorable HIA and QED scores, suggesting that, despite their promising scaffolds, these compounds would require pharmacokinetic optimization. **TSC1** and **TSC3** presented MEC-18 values close to the threshold, being considered less structurally "innovative," yet they exhibited good QED and low HIA values.

Although *ortho*-naphthoquinone **4** shows a high MEC-18 value (62.7) and elevated HIA (0.937), it exhibits a low QED (0.402) and high CL_{plasma}. In contrast, β-lapachone-3-sulfonic acid (**3**) combines a high MEC-18 value (72.6) with a favorable QED (0.623), high HIA (0.964), and moderate plasma clearance, making it the candidate with the best balance between structural innovation and pharmacokinetic profile.

3. Materials and Methods

3.1. Materials

All chemicals were purchased from commercial suppliers and used without further purification. Melting points (mp) were determined through a PFM-II (Instrumentation MS Tecnopon®, Piracicaba, São Paulo, Brazil) melting-point apparatus. The purity of the synthesized compounds was determined by thin-layer chromatography (TLC) (Sulpeco Analitical, Germany) using several solvent systems of different polarities. NMR spectra were recorded on a Bruker Ascend 400 spectrometer (Bruker, Billerica, Massachusetts, USA), operating at 400 MHz for ^{1}H NMR and 100 MHz for ^{13}C NMR. $CDCl_3$ and DMSO-d_6 were used as solvents with tetramethylsilane (TMS) as the internal standard; chemical shifts (δ) are given in ppm and coupling constants (*J*) in Hz. Mass spectra were recorded with a Bruker Daltonics (TOF-Q-II) spectrometer (Bruker, Billerica, Massachusetts, USA) using electrospray ionization.

3.2. Synthesis

3.2.1. Extraction of 2-Hydroxy-3-(3-methyl-2-butenyl)-1,4-naphthoquinone (**1**)

Lapachol (**1**) was isolated from the heartwood of *Tabebuia* sp. Wood splinters were immersed in 1% (*w*/*v*) sodium hydroxide (NaOH) aqueous solution and kept for 24 h. The resulting mixture was filtered, and the filtrate was acidified with 6 M hydrochloric acid (HCl), leading to the precipitation of lapachol (**1**) as a yellow solid. The precipitate was collected by vacuum filtration and dried at room temperature [16]. Lapachol (**1**) was purified by crystallization from 2:1 ethanol/water mixture. Yellow crystalline solid, yield: 1.5% *w*/*w*, mp: 138.3–140.3 °C. ^{1}H NMR (400 MHz, $CDCl_3$) δ: 8.12 (m, 1H, H5), 8.07 (m, 1H, H8), 7.75 (td, *J* = 7.6 and 1.4 Hz, 1H, H6), 7.67 (td, *J* = 7.5 and 1.4 Hz, 1H, H7), 7.33 (s, 1H, -OH), 5.21 (m, 1H, H10), 3.31 (d, *J* = 7.4 Hz, 2H, -CH_2), 1.79 (s, 3H, -CH_3), 1.69 (s, 3H, -CH_3). ^{13}C NMR (100 MHz, $CDCl_3$) δ: 184.6 (C4), 181.7 (C1), 152.7 (C2), 134.9 (C6), 133.9 (C4a and C11), 132.9 (C7), 129.4 (C8a), 126.8 (C5), 126.1 (C8), 123.4 (C3), 119.6 (C10), 25.8 (-CH_3), 22.6 (C9), 17.9 (-CH_3), HRMS (ES+) calculated for $C_{15}H_{14}O_3$ [M+H]+: 242.0943 and in literature FAB-MS: *m*/*z* 243 [26].

3.2.2. Synthesis of 3,4-Dihydro-2,2-dimethyl-2*H*-naphtho [1,2-b]pyran-5,6-dione (**2**)

In a 25 mL reaction flask, lapachol (**1**) (484 mg, 2 mmol) was weighed and added to concentrated sulfuric acid (H_2SO_4) solution (5 mL). The reaction mixture was stirred at room temperature for 1.0 h, then poured into 400 mL of ice-cold deionized water. The solid obtained was vacuum filtered and allowed to dry at room temperature, which resulting in a yield of 95% [4]. Orange solid, mp: 155 °C. ^{1}H NMR (400 MHz, DMSO-d_6) δ [ppm]: 7.91 (d, *J* = 7.6 Hz, 1H), 7.77 (m, 2H), 7.61 (m, 1H), 2.40 (t, *J* = 6.6 Hz, 2H), 1.82 (t, *J* = 6.6 Hz, 2H), 1.43 (s, 6H). ^{13}C NMR (100 MHz DMSO-d_6) δ (ppm): 179.1, 177.8, 160.6, 135.0, 132.1, 130.8, 129.9, 127.8, 123.7, 112.5, 79.0, 30.8, 26.3, 15.9 (Figure S1). HRMS (ES+) calculated for $C_{15}H_{14}O_3$ [M+H]+: 242.0943 and in literature FAB-MS: *m*/*z* 243 [27].

3.2.3. Synthesis of 3,4,5,6-Tetrahydro-2,2-dimethyl-5,6-dioxo-2*H*-naphtho[1,2-b]pyran-3-sulfonic acid (**3**)

Lapachol (**1**) (242 mg, 1.0 mmol) was weighed into a 25 mL round-bottom flask and cooled in an ice bath (5–16 °C). Cold acetic anhydride (Ac_2O; 1.5 mL) was then added, and the resulting suspension was stirred while concentrated sulfuric acid (H_2SO_4, 160 µL) was added dropwise. The reaction mixture was kept under stirring in an ice bath until complete consumption of lapachol (**1**), and monitoring was performed by TLC (2.0 h). A solid precipitate formed in the reaction medium, which was collected by filtration, washed with cold ethyl ether (three times, 20 mL each), and dried at room temperature [17]. Red solid, yield: 80%; mp: 168–170 °C. ^{1}H NMR (400 MHz, DMSO-d_6) δ 7.9 (dt, *J* = 7.7 Hz, *J* = 1.2 Hz, 1H), 7.7 (m, 2H), 7.6 (m, 1H), 2.8 (m, 2H), 2.5 (m, 1H), 1.7 (s, 3H), 1.4 (s, 3H). ^{13}C NMR (100 MHz, DMSO-d_6) δ 177.6 (C1), 179.1 (C2), 130.0 (C3), 131.9 (C4), 169.8 (C5), 111.8 (C6), 123.8 (C7), 135.0 (C8), 130.8 (C9), 127.8 (C10), 82.0 (C11), 59.2 (C12), 20.5 (C13a), 20.5 (C13b), 21.1 (C14), 28.4 (C15) (Figure S2). HRMS (ES+) calculated for $C_{15}H_{14}O_3$ $[M+H]^+$: 322.0511 and in literature EM (ES-): 321.2 [28].

3.2.4. Synthesis of 3,4-Dihydro-3-iodo-2,2-dimethyl-2*H*-naphtho[1,2-b]pyran-5,6-dione (**4**)

3-Iodo-β-lapachone (**4**) was synthesized via iodination of lapachol (**1**) in basic medium. Lapachol (**1**) (484 mg, 2.0 mmol) was dissolved in dichloromethane (40 mL), after which iodo (504 mg, 4.0 mmol) and pyridine (95 mg, 1.2 mmol) were added. The reaction mixture was stirred at room temperature for 24 h. After completion, the solvent was allowed to evaporate under ambient conditions, yielding a dark paste, which was treated with absolute ethanol (3.0 mL) and sonicated for 180 s, yielding a dark orange precipitate. The solid

was isolated by filtration and dried at room temperature. Purification was performed by column chromatography using a progressively polar elution system [17]. Orange crystalline solid, yield: 20%; mp: 130–131 °C. ^{1}H NMR (400 MHz, DMSO-d_6) δ 7.95 (d, *J* = 7.5 Hz, 1H,), 7.83–7.76 (m, 2H), 7.69–7.62 (m, 1H), 4.73 (t, *J* = 5.8 Hz, 1H), 3.20 (dd, *J* = 18.2 and 5.3 Hz, 1H), 2.98 (dd, *J* = 18.2 and 6.3 Hz, 1H), 1.60 (s, 3H), 1.59 (s, 3H). ^{13}C NMR (100 MHz, DMSO-d_6) δ 179.0, 177.8, 160.3, 135.6, 131.9, 131.7, 130.4, 128.5, 124.3, 112.0, 81.2, 30.9, 30.7, 27.4, 25.1 (Figures S3). HRMS (ES+) calculated for $C_{15}H_{13}IO_3$ $[M+H]^+$: 367.9909 and in literature EM (ES+): 367.9909 [29].

3.2.5. Synthesis of Thiosemicarbazones (**TSC1** and **TSC2**)

An ethanolic solution (6 mL) of the appropriate naphthoquinone (**2** or **3**, 1 mmol) was heated to 70 °C and acidified with two drops of concentrated HCl. Thiosemicarbazide (1 mmol) was then added, and the mixture kept under stirring and heating for 2 h, with the reaction progress monitored by TLC. After completion, the mixture was cooled to room temperature and brought to pH 7 using 5% sodium carbonate (Na_2CO_3) aqueous solution. For the synthesis of **TSC2**, neutralization was performed with triethylamine instead. Further cooling induced complete precipitation of the product. The solids were collected by filtration, washed with water, and dried at room temperature.

(*Z*)-2-(2,2-dimethyl-5-oxo-3,4-dihydro-2*H*-benzo[h]chromen-6(5*H*)-ylidene)hydrazine-1-carbothioamide (**TSC1**)—orange solid; yield: 72%; mp: 214–216 °C. ^{1}H NMR (400 MHz, DMSO-d_6) δ 14.9 (s, 1H), 9.2 (s, 1H), 9.0 (s, 1H), 8.6 (dd, *J* = 6.0, 3.2 Hz, 1H), 7.8 (dd, *J* = 6.1 and 3.1 Hz, 1H), 7.6–7.5 (m, 2H), 2.5 (dd, *J* = 6.8 and 6.8 Hz, 2H), 1.8 (t, *J* = 6.8 Hz, 2H), 1.4 (s, 6H). ^{13}C RMN (100 MHz, DMSO-d_6): δ 181.2 (C5), 180.0 (C13), 161.6 (C1a), 131.6 (C6a↔C10a), 130.4 (C9↔C10), 129.7 (C6), 129.3 (C9↔C10), 126.7 (C6a↔C10a), 124.7 (C8), 123.2 (C7), 111.9 (C4a), 79.2 (C2), 31,3 (C3), 26.8 (C11 e C12), 16.2 (C4). HRMS (ES+) calculated for $C_{16}H_{17}N_3O_2S$ $[M+H]^+$: 316.1041. Found: 316.1145 (Figure S4).

(*Z*)-6-(2-carbamothioylhydrazono)-2,2-dimethyl-5-oxo-3,4,5,6-tetrahydro-2*H*-benzo[h]-chromene-3-sulfonic acid (**TSC2**)—red solid; yield: 62%; dec. 228–230 °C. ^{1}H NMR (400 MHz, DMSO-d_6) δ 14.9 (s, 1H), 9.2 (s, 1H), 9.0 (s, 1H), 8.6 (s, 1H), 7.8 (s, 1H), 7.5 (s, 2H), 2.9 (dd, *J* = 41.2 and 14.6 Hz, 2H), 2.6 (m, 1H), 1.8 (s, 3H), 1.4 (s, 3H). ^{13}C RMN (100 MHz, DMSO-d6): δ 180.9 (C13), 180.1 (C5), 160.8 (C1a), 131.5 (C6a↔C10a), 130.5 (C9↔C10), 129.8 (C9↔C10), 129.3 (C9↔C10), 126.5 (C6), 124.7 (C7), 123.4 (C8), 112.2 (C4a), 82.1 (C2), 59.9 (C3), 29.1 (C11↔C12), 21.5 (C11↔C12), 20.8 (C4). HRMS (ES+) calculated for $C_{16}H_{17}N_3O_5S_2$ $[M+H]^+$: 396.0643. Found: 396.0717 (Figure S5).

3.2.6. Synthesis of Methylthiosemicarbazones (**TSC3**, **TSC4** and **TSC5**)

A methanolic solution (6 mL) containing the appropriate naphthoquinone (**2**, **3** or **4**, 1.0 mmol) and 4-methyl-3-thiosemicarbazide (1.0 mmol) was heated to 70 °C and acidified with two drops of concentrated HCl. For the synthesis of **TSC5**, 1mmol of sodium acetate (NaOAc) was employed as a catalyst. The reaction mixture was maintained under stirring and heating for 2 h, and the progress was monitored by TLC to confirm the consumption of the naphthoquinone. Upon completion, the precipitated solid was collected by filtration, washed with methanol, and dried at room temperature.

(*Z*)-2-(2,2-dimethyl-5-oxo-3,4-dihydro-2*H*-benzo[h]chromen-6(5*H*)-ylidene)-N-methyl-hydrazine-1-carbothioamide (**TSC3**)—orange solid; yield 87%; mp: 218–219 °C. ^{1}H NMR (400 MHz, $CDCl_3$): δ 15.1 (s, 1H), 8.1–8.0 (m, 1H, H10), 8.0 (d, *J* = 3.6 Hz, 1H, NH), 7.9 (dd, *J* = 8.2 and 6.0 Hz, 2H, H7), 7.5–7.4 (m, 2H, H8 and H9); 3.3 (d, *J* = 4.9 Hz, 3H, H15), 2.6 (t, *J* = 6.7 Hz, 3H, H4), 1.8 (t, *J* = 6.7 Hz, 3H, H3), 1.45 (s, 6H, H16 and H17). ^{13}C NMR (100 MHz, $CDCl_3$): δ [ppm] 181.1 (C5); 179.8 (C13); 161.5 (C1a); 131.4 (C6a); 129.7 (C9); 129.2 (C6); 128.6 (C8); 127.2 (C10a); 123.5 (C7); 122.7 (C10); 111.6 (C4a); 78.5 (C2); 31.7 (C3);

31.5 (C15); 27.1 (C16 and C17); 16.1 (C4). HRMS (ES+) calculated for $C_{17}H_{19}N_3O_2S$ $[M+H]^+$: 330.1232. Found: 330.1299 (Figure S6).

(*Z*)-2,2-dimethyl-6-(2-(methylcarbamothioyl)hydrazono)-5-oxo-3,4,5,6-tetrahydro-2*H*-benzo[h]chromene-3-sulfonic acid (**TSC4**)—yellow solid; yield 73%; it decomposed at 250 °C. ^{1}H NMR (400 MHz, DMSO-d_6): δ 15.0 (s, 1H, C=N–NH), 9.5 (d, *J* = 3.9 Hz, 1H, SC–NH), 8.6–8.5 (m, 1H, H7), 7.8–7.7 (m, 1H, H10), 7.6–7.5 (m, 2H, H8 and H9), 3.13 (d, *J* = 3.7 Hz, 3H, H15), 2.9 (dd, *J* = 17.5 and 5.2 Hz, 1H, H4), 2.8 (dd, *J* = 11.8 and 5.2 Hz, 1H, H3), 2.5 (dd, *J* = 14.0 and 8.4 Hz, 1H, H4), 1.8 (s, 3H, H17); 1.4 (s, 3H, H16). ^{13}C NMR (100 MHz, DMSO-d_6): δ 180.9 (C5), 178.7 (C13), 160.6 (C1a), 131.5 (C6a), 130.3 (C8↔C9), 129.4 (C6), 129.2 (C8↔C9), 126.4 (C6), 124.5 (C7), 123.4 (C10), 112.3 (C4a), 82.0 (C2), 60,0 (C3), 32.2 (C15), 29.2 (C16↔C17), 21.4 (C16↔C17); 20.8 (C3). HRMS (ES+) calculated for $C_{17}H_{19}N_3O_5S_2$ $[M+H]^+$: 410.0800. Found: 410.0873 (Figure S7).

(*Z*)-2-(3-iodo-2,2-dimethyl-5-oxo-3,4-dihydro-2*H*-benzo[h]chromen-6(5*H*)-ylidene)-N-methylhydrazine-1-carbothioamide (**TSC5**)—orange solid; yield 63%; mp: 191–192 °C. ^{1}H NMR (400 MHz, $CDCl_3$): δ 15.0 (s, 1H, C=N–NH), 8.1 (d, *J* = 7.0 Hz, 1H, H7), 8.0 (s, 1H, SC–NH), 7.9 (d, *J* = 7.4 Hz, 1H, H10), 7.6–7.4 (m, 2H, H8 and H9), 4.4 (t, *J* = 6.7 Hz, 1H, H3), 3.3 (d, *J* = 3.9 Hz, 4H, H4 and H15), 3.2 (dd, *J* = 17.9 and 8.6 Hz, 1H, H4), 1.7 (s, 3H, H16), 1.6 (s, 3H, H17). ^{13}C NMR (100 MHz, $CDCl_3$): δ 179.6 (C5), 179.0 (C13), 160.0 (C1a), 130.2 (C8, C9), 128.7 (C8, C9), 123.6 (C10), 122.8 (C7), 110.5 (C1a), 80.6 (C2), 31.5 (C15), 30.5 (C4), 29.0 (C3), 26.9 (C16↔C17). HRMS (ES+) calculated for $C_{17}H_{18}IN_3O_2S$ [M+H]+: 456.0198. Found: 456.0269 (Figure S8).

3.2.7. Synthesis of Phenylthiosemicarbazone (**TSC6**)

A methanolic solution (12 mL) containing β-lapachone-3-sulfonic acid (**3**, 1.0 mmol), 4-phenyl-3-thiosemicarbazide (1.0 mmol) and sodium acetate (NaOAc, 1.0 mmol) was heated to 70 °C. The reaction mixture was stirred and heated for 6 h, and the progress was monitored by TLC to confirm the consumption of the naphthoquinone **3**. Upon completion, the resulting precipitate was collected by filtration, washed with ethyl acetate, and dried at room temperature.

(Z)-2,2-dimethyl-5-oxo-6-(2-(phenylcarbamothioyl)hydrazono)-3,4,5,6-tetrahydro-2*H*-benzo[h]chromene-3-sulfonic acid (**TSC6**)—orange solid; yield 13%; it decomposed at 270 °C. ^{1}H NMR (400 MHz, DMSO-d_6): δ 15.3 (s, 1H, N=NH), 11.0 (s, 1H, NH), 8.7 (s, 1H, H7), 7.8 (s, 1H, H10), 7.6 (d, *J* = 7.7 Hz, 2H, H20 and H16), 7.5 (d, *J* = 3.8 Hz, 2H, H17 and H19), 7.4 (t, *J* = 7.3 Hz, 2H, H8 and H9), 7.3 (t, *J* = 7.1 Hz, 1H, H18), 3.0 (d, *J* = 17.6 Hz, 1H, H4″), 2.8 (d, *J* = 11.7 Hz, 1H, H4′), 2.6–2.5 (m, 1H, H3), 1.8 (s, 3H, CH_3′), 1.4 (s, 3H, CH_3). ^{13}C NMR (100 MHz, DMSO-d_6): δ 181.1 (C5), 177.8 (C13), 160.8 (C1a), 139.1 (C6a↔C10a), 131.5 (C6a↔C10a), 130.4 (C17, C19), 130.2 (C6), 129.5 (C16↔C20), 128.9 (C8↔C9), 126.9 (C18), 126.7 (C16↔C20), 126.6 (C15), 125.0 (C7), 123.4 (C10), 112.3 (C4a), 82.2 (C2), 59.9 (C4), 29.2 (CH_3′↔CH_3), 21.5 (CH_3↔CH_3′), 20.8 (C3). HRMS (ES+) calculated for $C_{22}H_{21}N_3O_5S_2$ [M+H]+: 472.0956 Found: 472.1031 (Figure S9).

3.3. In Vitro Cytotoxicity Evaluation

The cell lines L929 (murine fibroblasts, ATCC® CCL-1™), B16–F10 (murine melanoma, ATCC® CRL-6475™), CT26.WT (murine colon carcinoma, ATCC® CRL-2638™), and 4T1 (murine breast cancer, ATCC® CRL-2539™) were kindly provided by the National Cancer Institute (Bethesda, MD, USA). Cells were cultured in Dulbecco's Modified Eagle's Medium DMEM (for L929) or RPMI-1640 (for B16-F10, CT26.WT, and 4T1) media, both supplemented with 10% fetal bovine serum (FBS) and 1% penicillin/streptomycin (Sigma Aldrich Co., St. Louis, MO, USA). Cultures were maintained in an incubator Shel Lab®

(Sellex Scientific, Inc, Kensington, MD, USA) at 37 °C under a humidified atmosphere containing 5% CO_2.

The compounds were dissolved in analytical-grade dimethyl sulfoxide (DMSO, Dinâmica®, Indaiatuba, SP, Brazil) to obtain stock solutions of 10 mg/mL. Working solutions were prepared to yield a final concentration of 25 µg/mL in culture medium. In our cell culture' research group, a concentration of 25 µL/mL is used for a 72 h screening cytotoxicity assay of natural, synthetic, or semi-synthetic substances. The negative control consisted of untreated cells, while doxorubicin (0.5 µg/mL) was used as the positive control.

Cytotoxicity Assay

Cytotoxicity was evaluated using the 3-(4,5-dimethylthiazol-2-yl)-2,5-diphenyltetrazolium bromide (MTT) assay, as described by Mosmann (1983) [30] and adapted by Skehan et al. (1990) [31]. This colorimetric method is based on the reduction of MTT to formazan crystals by mitochondrial enzymes present in metabolically active cells [32].

Cells were seeded at a density of 5×10^3 cells/mL in 96-well plates and incubated for 68 h at 37 °C in 5% CO_2 atmosphere. After incubation, 20 µL of MTT solution (prepared in sterile PBS) was added to each well, followed by a 4 h incubation period. The resulting formazan crystals were solubilized with 100 µL of DMSO, and the absorbance was measured at 560 nm using a GloMax 96 microplate reader (Promega, Madison, WI, USA). The results were presented as the percentage of cell proliferation inhibition (PI%) after 72 h of incubation. In evaluating the cytotoxic potential of the tested compounds, the scale described by Souza and collaborators (2016) was used. At this scale, the samples were classified as: no activity (PI% $\leq$ 0.00%); low activity (PI% from 1.00% to 50.00%); moderate activity (PI% from 50.00% to 75.00%); and high activity (PI% > 75.00%) [33].

All experiments were performed in triplicate, and results were expressed as mean ± standard deviation (SD) of the percentage of cell growth inhibition. Statistical analyses were carried out using OriginPRO® 2025 Program (OriginLab® Corporation, Northampton, MA, USA). Data were analyzed by one-way analysis of variance (ANOVA) followed by Dunnett's post hoc test, with significance accepted at $p < 0.05$.

3.4. ADMET Predictions

Naphthoquinones and thiosemicarbazones were submitted to ADMETLab 3.0 software (available at https://admetlab3.scbdd.com/, accessed on 1 September 2025) for prediction of physicochemical and pharmacokinetic parameters such as MW, logS, logP, TPSA, QED, MEC-18, Caco-2 permeability, HIA, PPB, and CL_{plasma}.

4. Conclusions

A series of β-lapachone-based thiosemicarbazones (**TSC1**–**TSC6**) was successfully synthesized from naturally obtained lapachol (**1**) via straightforward, efficient routes. The synthetic procedures afforded good to excellent yields for the *ortho*-naphthoquinone intermediates (compounds **2**, **3** and **4**) and moderate yields for their thiosemicarbazone derivatives. Naphthoquinone **2** exhibited high cytotoxicity against the evaluated tumor cell lines, with a moderate effect on normal cells. Its derivatives, **TSC1** and **TSC3**, showed lower inhibition of tumor cell proliferation compared to compound **2**; however, they displayed greater selectivity, a desirable feature in antineoplastic compounds. Compound **3** stood out for its marked cytotoxicity against melanoma and breast cancer cells, combined with low toxicity toward normal cells, indicating potential tumor selectivity. In contrast, the thiosemicarbazones **TSC2**, **TSC4**, and **TSC6**, derived from the *ortho*-naphthoquinone **3**, exhibited reduced or no antiproliferative activity. Compound **4** displayed high toxicity toward both tumor and normal cell lines, suggesting low selectivity. Conversely, its

derivative, thiosemicarbazone **TSC5**, demonstrated moderate antiproliferative activity against melanoma cells and low cytotoxicity toward normal fibroblasts, revealing a safer and more promising profile. Overall, the introduction of the thiosemicarbazone group conferred more attractive antitumor properties to derivatives **TSC1**, **TSC3**, and **TSC5** compared to their naphthoquinone precursors (**2** and **4**). Compounds **2**, **3**, **TSC1**, and **TSC3** also exhibited favorable pharmacokinetic profiles (QED ≈ 0.61–0.66), with balanced lipophilicity and adequate solubility, suggesting good oral bioavailability. Among them, compound **3** stands out as the most promising candidate, combining high tumor selectivity, suitable ADME parameters, and an innovative structure (MEC-18 = 72.6). The results highlight the potential of naphthoquinone **3** and thiosemicarbazones **TSC1** and **TSC3** as lead compounds for further optimization and development of new antineoplastic agents with improved pharmacokinetic and safety profiles.

Supplementary Materials: The following supporting information can be downloaded at: https://www.mdpi.com/article/10.3390/ddc5010001/s1, Figure S1. ^{1}H and ^{13}C one- and two-dimensional NMR spectra and high-resolution mass spectra of β-lapachone (**2**); Figure S2. ^{1}H and ^{13}C one- and two-dimensional NMR spectra and high-resolution mass spectra of β-Lapachone-3-Sulfonic Acid (**3**); Figure S3. ^{1}H and ^{13}C one- and two-dimensional NMR spectra and high-resolution mass spectra of 3-iodo-β-lapachone (**4**); Figure S4. ^{1}H and ^{13}C one- and two-dimensional NMR spectra and high-resolution mass spectra of (*Z*)-2-(2,2-dimethyl-5-oxo-3,4-dihydro-2*H*-benzo[h]chromen-6(5*H*)-ylidene)hydrazine-1-carbothioamide (**TSC1**); Figure S5. ^{1}H and ^{13}C one- and two-dimensional NMR spectra and high-resolution mass spectra of (*Z*)-6-(2-carbamothioylhydrazono)-2,2-dimethyl-5-oxo-3,4,5,6-tetrahydro-2*H*-benzo[h]chromene-3-sulfonic acid (**TSC2**); Figure S6. ^{1}H and ^{13}C one- and two-dimensional NMR spectra and high-resolution mass spectra of (*Z*)-2-(2,2-dimethyl-5-oxo-3,4-dihydro-2*H*-benzo[h]chromen-6(5*H*)-ylidene)-N-methylhydrazine-1-carbothioamide (**TSC3**); Figure S7. ^{1}H and ^{13}C one- and two-dimensional NMR spectra and high-resolution mass spectra of (*Z*)-2,2-dimethyl-6-(2-(methylcarbamothioyl)hydrazono)-5-oxo-3,4,5,6-tetrahydro-2*H*-benzo[h]chromene-3-sulfonic acid (**TSC4**); Figure S8. ^{1}H and ^{13}C one- and two-dimensional NMR spectra and high-resolution mass spectra of (*Z*)-2-(3-iodo-2,2-dimethyl-5-oxo-3,4-dihydro-2*H*-benzo[h]chromen-6(5*H*)-ylidene)-N-methylhydrazine-1-carbothioamide (**TSC5**); and Figure S9. ^{1}H and ^{13}C one- and two-dimensional NMR spectra and high-resolution mass spectra of (Z)-2,2-dimethyl-5-oxo-6-(2-(phenylcarbamothioyl)hydrazono)-3,4,5,6-tetrahydro-2*H*-benzo[h]chromene-3-sulfonic acid (**TSC6**). Table S1. Mean proliferation inhibition values from the MTT assays of each replicate.

Author Contributions: Conceptualization, C.R.M.A. and M.P.d.C.; Methodology, E.S.d.S., E.A.d.S., I.L.S.d.S., P.M.P.F. and R.W.R.d.S.; Software, M.P.d.C.; Validation, C.R.M.A. and M.P.d.C.; Formal Analysis, A.d.A.G., P.M.P.F. and R.W.R.d.S.; Investigation, E.S.d.S., E.A.d.S., I.L.S.d.S., P.M.P.F. and R.W.R.d.S.; Resources, E.S.d.S., E.A.d.S., I.L.S.d.S., P.M.P.F. and R.W.R.d.S.; Writing—Original Draft Preparation, C.R.M.A.; Writing—Review and Editing, E.S.d.S., E.A.d.S., D.G.G., A.d.A.G., C.R.M.A. and M.P.d.C.; Supervision, C.R.M.A.; Project Administration, C.R.M.A.; Funding Acquisition, C.R.M.A. All authors have read and agreed to the published version of the manuscript.

Funding: This research was funded by Coordenação de Aperfeiçoamento de Pessoal de Nível Superior—CAPES, grant number 001 and Fundação de Amparo à Ciência e Tecnologia do Estado de Pernambuco—FACEPE, grant numbers: APQ-0184-1.06/24 and IBPG-1814-4.00/22.

Institutional Review Board Statement: Not applicable.

Informed Consent Statement: Not applicable.

Data Availability Statement: The original contributions presented in this study are included in the article/Supplementary Material. Further inquiries can be directed to the corresponding author.

Acknowledgments: This research utilized facilities at the National Laboratory of Biofuels (LNBR), part of the National Center for Research in Energy and Materials (CNPEM), a Social Organization supervised by the Ministry of Science, Technology and Innovation (MCTI). The Metabolomics facility team is recognized for its assistance during the experiments proposed in project 20233066.

Conflicts of Interest: The authors declare no conflicts of interest. The funders had no role in the design of the study; in the collection, analyses, or interpretation of data; in the writing of the manuscript; or in the decision to publish the results.

Abbreviations

The following abbreviations are used in this manuscript:

ADME	Absorption, distribution, metabolism, and excretion
CL_{plasma}	Plasma clearance
FBS	Fetal bovine serum
FDA	Food and Drug Administration
HIA	Human intestinal absorption
LogP	Logarithm of the n-octanol/water distribution coefficients
LogS	Logarithm of aqueous solubility value
MEC-18	Minimum energy conformation at 18 descriptors
mp	Melting point
MTT	3-(4,5-dimethylthiazol-2-yl)-2,5-diphenyltetrazolium bromide
MW	Molecular weight
NMR	Nuclear Magnetic Resonance
PPB	Plasma protein binding
QED	Quantitative estimate of drug-likeness
R&D	Research and development
TLC	Thin-layer chromatography
TPSA	Topological polar surface area

References

1. Novel Drug Approvals for 2024. Available online: https://www.fda.gov/media/184967/download?attachment (accessed on 20 November 2025).
2. Harrison, R. Phase II and phase III failures: 2013–2015. *Nat. Rev. Drug Discov.* **2016**, *15*, 817–818. [CrossRef]
3. Gupta, U.C.; Bhatia, S.; Garg, A.; Sharma, A.; Choudhary, V. Phase 0 clinical trials in oncology new drug development. *Perspect. Clin. Res.* **2011**, *2*, 13–22. [CrossRef]
4. Santos, V.L.d.A.; Gonsalves, A.d.A.; Guimarães, D.G.; Simplicio, S.S.; Oliveira, H.P.d.; Ramos, L.P.S.; Costa, M.P.d.; Oliveira, F.d.C.E.d.; Pessoa, C.; Araújo, C.R.M. Naphth[1,2-d]imidazoles Bioactive from β-Lapachone: Fluorescent Probes and Cytotoxic Agents to Cancer Cells. *Molecules* **2023**, *28*, 3008. [CrossRef]
5. Castellanos, J.R.G.; Prieto, J.M.; Heinrich, M. Red Lapacho (Tabebuia impetiginosa)—A global ethnopharmacological commodity? *J. Ethnopharmacol.* **2009**, *121*, 1–13. [CrossRef]
6. Li, Y.; Sun, X.; LaMont, J.T.; Pardee, A.B.; Li, C.J. Selective killing of cancer cells by beta -lapachone: Direct checkpoint activation as a strategy against cancer. *Proc. Natl. Acad. Sci. USA* **2003**, *100*, 2674–2678. [CrossRef]
7. Seville, L.L.; Shah, N.; Westwell, A.D.; Chan, W.C. Modulation of pRb/E2F Functions in the Regulation of Cell Cycle and in Cancer. *Curr. Cancer Drug Targets* **2005**, *5*, 159–170. [CrossRef] [PubMed]
8. Shapiro, G.I.; Supko, J.G.; Ryan, D.P.; Appelman, L.; Berkenblit, A.; Craig, A.R.; Jones, S.; Yagovane, D.; Li, C.; Eder, J. Phase I trial of ARQ 501, an Activated Checkpoint Therapy (ACT) agent, in patients with advanced solid tumors. *J. Clin. Oncol.* **2005**, *23*, 3042. [CrossRef]
9. Li, C.; Nemunaitis, J.; Senzer, N.; Edelman, G.; Glasner, S.; Dombal, G.; Dovholuk, A.; Cunningham, C. A phase Ib trial of ARQ 501, a selective checkpoint activator, in combination with docetaxel in patients with advanced solid tumors. *J. Clin. Oncol.* **2006**, *24*, 13053. [CrossRef]
10. Kawecki, A.; Adkins, D.R.; Cunningham, C.C.; Vokes, E.; Yagovane, D.M.; Dombal, G.; Koralewski, P.; Hotko, Y.; Vladimirov, V. A phase II study of ARQ 501 in patients with advanced squamous cell carcinoma of the head and neck. *J. Clin. Oncol.* **2007**, *25*, 16509. [CrossRef]

11. Khong, H.T.; Dreisbach, L.; Kindler, H.L.; Trent, D.F.; Jeziorski, K.G.; Bonderenko, I.; Popiela, T.; Yagovane, D.M.; Dombal, G. A phase 2 study of ARQ 501 in combination with gemcitabine in adult patients with treatment naïve, unresectable pancreatic adenocarcinoma. *J. Clin. Oncol.* **2007**, *25*, 15017. [CrossRef]
12. Kunos, C.A.; Chu, E.; Beumer, J.H.; Sznol, M.; Ivy, S.P. Phase I trial of daily triapine in combination with cisplatin chemotherapy for advanced-stage malignancies. *Cancer Chemother. Pharmacol.* **2017**, *79*, 201–207. [CrossRef] [PubMed]
13. Kunos, C.A.; Radivoyevitch, T.; Waggoner, S.; Debernardo, R.; Zanotti, K.; Resnick, K.; Fusco, N.; Adams, R.; Redline, R.; Faulhaber, P.; et al. Radiochemotherapy plus 3-aminopyridine-2-carboxaldehyde thiosemicarbazone (3-AP, NSC #663249) in advanced-stage cervical and vaginal cancers. *Gynecol. Oncol.* **2013**, *130*, 75–80. [CrossRef]
14. Leath, C.A.; Deng, W.; Mell, L.K.; Richardson, D.L.; Walker, J.L.; Holman, L.L.; Lea, J.S.; Amarnath, S.R.; Santo-Reyes, L.J.; Arend, R.C.; et al. Incorporation of triapine (T) to cisplatin chemoradiation (CRT) for locally advanced cervical and vaginal cancer: Results from NRG-GY006, a phase III randomized trial. *Gynecol. Oncol.* **2025**, *195*, 122–133. [CrossRef]
15. Zeidner, J.F.; Karp, J.E.; Blackford, A.L.; Smith, B.D.; Gojo, I.; Gore, S.D.; Levis, M.J.; Carraway, H.E.; Greer, J.M.; Ivy, S.P.; et al. A phase II trial of sequential ribonucleotide reductase inhibition in aggressive myeloproliferative neoplasms. *Haematologica* **2014**, *99*, 672–678. [CrossRef]
16. Guimarães, D.G.; Santos, V.L.A.; Simplicio, S.S.; Gonsalves, A.A.; Gouveia, J.J.S.; Gusmão, F.B.A.A.; Tedesco, A.C.; Primo, F.L.; Rolim, L.A.; Araújo, C.R.M. Naphthoxazoles Derived from Lapachol as Fluorescent DNA Probes: Synthesis and Binding Studies with Calf Thymus DNA. *J. Braz. Chem. Soc.* **2025**, *36*, e-20240188. [CrossRef]
17. Campos, W.R.A.; Costa, M.M.d.; Rosa, D.S.; Gonsalves, A.d.A.; Araújo, C.R.M. Antimicrobial Activity of Lapachol-Based Semicarbazones Against Drug-Resistant Bacterial Strains and in Silico ADMET Evaluation. *Braz. Arch. Biol. Technol.* **2024**, *67*, e24240053. [CrossRef]
18. Guimarães, D.G.; de Assis Gonsalves, A.; Rolim, L.A.; Araújo, E.C.; Dos Anjos Santos, V.L.; Silva, M.F.S.; de Cássia Evangelista de Oliveira, F.; da Costa, M.P.; Pessoa, C.; Fonseca Goulart, M.O.; et al. Naphthoquinone-based Hydrazone Hybrids: Synthesis and Potent Activity Against Cancer Cell Lines. *Med. Chem.* **2021**, *17*, 945–955. [CrossRef] [PubMed]
19. Hartner, L.P.; Rosen, L.; Hensley, M.; Mendelson, D.; Staddon, A.P.; Chow, W.; Kovalyov, O.; Ruka, W.; Skladowski, K.; Jagiello-Gruszfeld, A.; et al. Phase 2 dose multi-center, open-label study of ARQ 501, a checkpoint activator, in adult patients with persistent, recurrent or metastatic leiomyosarcoma (LMS). *J. Clin. Oncol.* **2007**, *25*, 20521. [CrossRef]
20. Xiong, G.; Wu, Z.; Yi, J.; Fu, L.; Yang, Z.; Hsieh, C.; Yin, M.; Zeng, X.; Wu, C.; Lu, A.; et al. ADMETlab 2.0: An integrated online platform for accurate and comprehensive predictions of ADMET properties. *Nucleic Acids Res.* **2021**, *49*, W5–W14. [CrossRef]
21. Fu, L.; Shi, S.; Yi, J.; Wang, N.; He, Y.; Wu, Z.; Peng, J.; Deng, Y.; Wang, W.; Wu, C.; et al. ADMETlab 3.0: An updated comprehensive online ADMET prediction platform enhanced with broader coverage, improved performance, API functionality and decision support. *Nucleic Acids Res.* **2024**, *52*, W422–W431. [CrossRef]
22. Bickerton, G.; Paolini, G.; Besnard, J.; Muresan, S.; Hopkins, A.L. Quantifying the chemical beauty of drugs. *Nat. Chem.* **2012**, *4*, 90–98. [CrossRef] [PubMed]
23. Lipinski, C.A.; Lombardo, F.; Dominy, B.W.; Feeney, P.J. Experimental and computational approaches to estimate solubility and permeability in drug discovery and development settings. *Adv. Drug Deliv. Rev.* **2001**, *46*, 3–26. [CrossRef] [PubMed]
24. Waring, M.J. Defining optimum lipophilicity and molecular weight ranges for drug candidates. *Bioorg. Med. Chem. Lett.* **2009**, *15*, 2844–2851. [CrossRef]
25. Ivanenkov, Y.A.; Zagribelnyy, B.A.; Aladinskiy, V.A. Are We Opening the Door to a New Era of Medicinal Chemistry or Being Collapsed to a Chemical Singularity? *J. Med. Chem.* **2019**, *62*, 10026–10043. [CrossRef]
26. Park, B.S.; Lee, H.K.; Lee, S.E.; Piao, X.L.; Takeoka, G.R.; Wong, R.Y.; Ahn, Y.J.; Kim, J.H. Antibacterial activity of Tabebuia impetiginosa Martius ex DC (Taheebo) against Helicobacter pylori. *J. Ethnopharmacol.* **2006**, *105*, 255–262. [CrossRef] [PubMed]
27. Claessens, S.; Habonimana, P.; De Kimpe, N. Synthesis of naturally occurring naphthoquinone epoxides and application in the synthesis of beta-lapachone. *Org. Biomol. Chem.* **2010**, *16*, 3790–3795. [CrossRef]
28. Souza, M.A.A.; Silva, A.R.; Ferreira, M.A.; Lemos, M.J.; Ramos, R.G.; Ferreira, A.B.B.; Souza, S.R. Biological activity of lapachol and some derivatives as antifungal and in seed germination. *Quim. Nova* **2008**, *31*, 1670–1672. [CrossRef]
29. Anaissi-Afonso, L.; Oramas-Royo, S.; Ayra-Plasencia, J.; Martin-Rodriguez, P.; Garcia-Luis, J.; Lorenzo-Castrillejo, I.; Fernandez-Perez, L.; Estevez-Braun, A.; Machin, F. Lawsone, Juglone, and β-Lapachone Derivatives with Enhanced Mitochondrial-Based Toxicity. *ACS Chem. Bio.* **2018**, *13*, 1950–1957. [CrossRef]
30. Mosmann, T. Rapid colorimetric assay for cellular growth and survival: Application to proliferation and cytotoxicity assays. *J. Immunol. Methods* **1983**, *65*, 55–63. [CrossRef]
31. Skehan, P.; Storeng, R.; Scudiero, D.; Monks, A.; McMahon, J.; Vistica, D.; Warren, J.T.; Bokesch, H.; Kenney, S.; Boyd, M.R. New colorimetric cytotoxicity assay for anticancer-drug screening. *J. Natl. Cancer Inst.* **1990**, *82*, 1107–1112. [CrossRef]

32. Berridge, M.V.; Tan, A.; McCoy, K.D.; Wang, R. The Biochemical and Cellular Basis of Cell Proliferation Assays That Use Tetrazolium Salts. *Biochemica* **1996**, *4*, 14–19.
33. Souza, L.G.S.; Almeida, M.C.S.; Lemos, T.L.G.; Ribeiro, P.R.V.; Brito, E.S.; Silva, V.L.M.; Silva, A.M.S.; Braz-Filho, R.; Costa, J.G.M.; Rodrigues, F.G.; et al. Synthesis, antibacterial and cytotoxic activities of new biflorin-based hydrazones and oximes. *Bioorg. Med. Chem. Lett.* **2016**, *26*, 435–439. [CrossRef] [PubMed]

Disclaimer/Publisher's Note: The statements, opinions and data contained in all publications are solely those of the individual author(s) and contributor(s) and not of MDPI and/or the editor(s). MDPI and/or the editor(s) disclaim responsibility for any injury to people or property resulting from any ideas, methods, instructions or products referred to in the content.